JCRS

Journal of Chemical Reactivity and Synthesis 2024: 14(1) 45-72

Research Article

Investigation of the performance of Fluorouracil and azathioprine anticancer drugs with SWNT and BNNT: Molecular and Quantum Mechanical Calculations

Fatemeh Moosavi[1], Neda Hasanzadeh[1*], Hooriye Yahyaei[2], Ayeh Rayatzadeh[1]

[1] Department of Chemistry, Ahvaz Branch, Islamic Azad University, Ahvaz, Iran.

[2] Department of Chemistry, Zanjan Branch, Islamic Azad University, Zanjan, Iran.

ARTICLE INFO:

Received:
24 September 2024

Accepted:
16 November 2024

Available online:
20 November 2024

✉: M. H. Farjam
nhzadeh_212@yahoo.com

ABSTRACT

This research investigated the interaction between two drugs fluorouracil (FLU) and azathioprine (AZA) (Pseudo Nucleotide Anticancer Drugs) with single-walled carbon nanotubes (SWCNTs) and boron nitride nanotubes (BNNTs) using molecular mechanics and quantum mechanics computational methods. The Self-Consistent Reaction Field (SCRF) method was utilized as a model and DFT as an analytical tool to delve into the AZA and FLU correlations with SWCNTs and BNNTs in different solvents. Additionally, the study analyzed the impacts of temperature on the stability of molecular bonds during the experiment. Frontier Molecular Orbital (FMO) analysis was performed on the compounds at the B3LYP/6-31+G* level. The interaction between drugs in SWCNT and BNNT was investigated using molecular mechanics methods in AMBER, OPLS, CHARMM, and MM+ force fields. The results indicate that boron nitride nanotubes (BNNTs) and pharmaceuticals interact better, pointing to BNNTs as a potential drug delivery system for biological cells.

Keywords: Pseudo Nucleotide Anticancer Drugs; Single-Wall Carbon Nanotubes (SWCNTs); Boron Nitride Nanotubes (BNNTs); Force Field

1. Introduction

The utilization of biocompatible and less toxic nanomaterials for the treatment of serious diseases like cancer has risen as a result of significant breakthroughs in nanotechnology [1]. The number of people affected by the prevalent and deadly disease known as cancer is rising. As a result, it is acknowledged as one of the most significant worldwide health issues [2].

In recent years, the preparation of nanoparticles as pharmaceutical nanocarriers has become very important [3]. The characteristic of nanoparticles is that they can store and protect drugs inside themselves and finally deliver them to the target cell [4-6].

Numerous strategies have been used to increase treatment efficiency and reduce the adverse effects of anticancer drugs [7]. There are several benefits to using nanotechnology-based approaches, including quick detection, precise localization of injured cells and their therapeutic effects, and targeting [1].

Anti-cancer chemotherapies treat a variety of cancer types, such as pancreatic, ovarian, lung, breast, stomach, and colon cancer, by using artificial or natural chemicals [8]. Azathioprine is now used in chemotherapy. It was once used to treat autoimmune diseases such as Crohn's disease, rheumatoid arthritis, and intestinal problems as well as transplant recipients by suppressing their immune reactions [9]. As an antagonist of purine metabolism, azathioprine reduces the number of T cells, prevents DNA, RNA, and protein production, and lowers the humoral and cellular immune systems activity. Furthermore, this drug may prevent mitotic division.

As an antimetabolite, Fluorouracil works by preventing the synthesis of proteins that are necessary for cell division and proliferation [10]. This process prevents uracil from becoming thymidylate, which by itself prevents DNA and RNA synthesis and eventually results in cell death [11]. These medications can quickly cross biological barriers and enter cell nuclei, where they impair cancer cells' DNA production and kill healthy cells. Due to their numerous

negative effects, these medications must be attached to nanotubes to deliver them specifically to specific cells [8].

Carbon nanotubes have this ability and can effectively pass through the cell membrane and biological barriers and quickly reach the cell nucleus [12]. In the studies conducted, CN nanotubes (CNTs) have received more attention from researchers because carbon nanotubes have high mechanical and thermal stability, large specific surface area, and sufficient chemical inertness [13].

In the field of drug delivery, the interaction of BN nanostructures with drug molecules be studied more [14, 15]. In extensive studies, some C atoms have been replaced by impurities such as N, B, and Si to produce other nanotubes [16-18].

Electronic structure and properties of boron nitride nanotubes were studied in interaction with 5-FU drug, as an anticancer drug. The results showed that the encapsulation and absorption of 5-FU molecules on the surface of BNNTs is a favorable process. As a result, BNNTs can be considered as a carrier for drug delivery and transport of 5-FU as an anticancer drug in biological systems [19]. The efficacy of drug delivery for hydroxyurea, mercaptopurine, and 5-fluorouracil was demonstrated to be outstanding when employing 8-connected ZIF (imidazolate framework) in a study conducted in 2017. Utilizing instantaneous image analysis and radial distribution functions (RDFs), it was discerned that the adsorption of drugs exhibits a predilection for the 6-membered ring pores within the ZIF structure. The findings suggest the potential utilization of ZIFs as a pH-sensitive modality for medication delivery [20].

In 2017, scientists explored the peptide-based MOFs structure as a nano-carrier for intelligent drug delivery using molecular dynamics simulations. It was demonstrated that the drug 5-fluorouracil interacts more strongly with the carriers at lower electric field intensities [20].

One of the most widely utilized nanostructures in medicine for targeted medication administration, imaging, and diagnostics is carbon nanotubes. Additionally, boron nitride nanotubes, which are composed of boron and nitrogen atoms, have superior solubility, thermal tolerance, and chemical resistance to oxidation compared to carbon nanotubes. They have a lot of potential for targeted medication delivery and cancer therapy since they are non-toxic and biocompatible [21]. Boron and nitrogen atoms were combined to create boron nitride nanotubes [22]. These nanotubes have the same structure as carbon nanotubes, but they have chemical resistance to oxidation due to their ionic properties and the relationship between boron and nitrogen. They are also more soluble and temperature-tolerant than carbon nanotubes, biocompatible, and have a great potential for drug administration due to their toxicity [23]. In this research, the interaction of fluorouracil (FLU) and azathioprine (AZA) (nucleotide-like anticancer drugs) with single-walled carbon nanotubes (SWCNTs) and boron nitride nanotubes (BNNTs) is investigated using molecular mechanics and quantum mechanics methods. Also, the interaction between drugs in SWCNT and BNNT is investigated using molecular mechanics methods in AMBER, OPLS, CHARMM, and MM+ force fields.

2. Computational Details

The Gaussian 09W computational framework was employed for conducting quantum chemical computations in this investigation [24, 25]. The molecular configurations of fluorouracil and Azathioprine (Fig 1-2), in conjunction with a singularly encapsulating single-walled nanotube and boron nitride, were systematically crafted using the GaussView software [26]. Subsequently, the requisite input file for the Gaussian program was generated to initiate quantum mechanical computations and optimization procedures. After these steps, the Gaussian program Theoretical calculations related to compounds were performed using B3LYP/6-31+G* level [27]. Evaluations were conducted on the Frontier Molecular Orbital

(FMO) characteristics, encompassing electrophilicity (ω), overall hardness properties (η), electronegativity (χ), electronic chemical potential (μ), and the HOMO-LUMO energy gap (Eg) [27-32].

The effects of the medication's fluorouracil and azathioprine on single-walled carbon nanotubes and boron nitride nanotubes at various temperatures were investigated using molecular mechanics simulations. The HyperChem [33] program was utilized for these computations, and the Monte Carlo approach was applied in a variety of areas, including AMBER [34], CHARM [35, 36], OPLS [37], and MM+ [38, 39]. The Monte Carlo method is a computer algorithm that computes results using statistical methods and random sampling. The dominating probability distribution is shown by the high level of matching between the simulated and actual systems [30, 40]. When using a deterministic algorithm to calculate results accurately is not practicable, this approach is typically employed. In addition, the Monte Carlo approach performs well when simulating continuous cross-sectional surfaces, various materials, and three-dimensional geometries [41, 42].

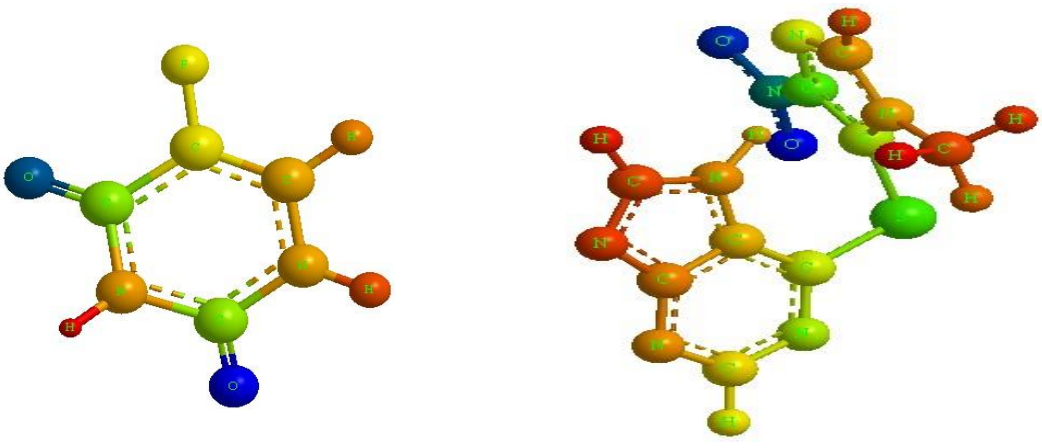

Fig. 1. Theoretical geometric structure of the FLU and AZA (optimized by B3LYP/6-31+G level).

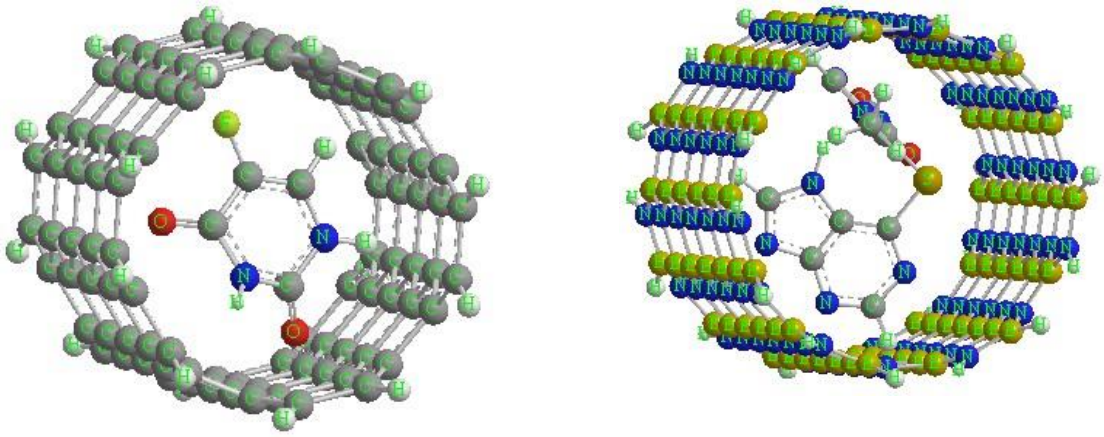

SWCNTS-FLU BNNTS-AZA

Fig. 2. Single-wall carbon Nanotubes (SWCNTs) and Boron Nitride Nanotubes (BNNTs) (optimized by B3LYP/6-31+G level).

3. Result and discussion

Molecular mechanics models molecular systems using classical mechanics [43]. It is predominantly employed in the realm of molecular dynamics, wherein a pertinent integral is harnessed for the emulation of particle trajectories and the anticipation of reaction pathways, while force fields are applied to delineate the exerted forces on individual particles [43]. The pursuit of energy minimization represents a distinctive domain within the realm of molecular mechanics application, wherein force fields serve as the evaluative criterion for the process of optimization [44]. This approach employs a judicious algorithmic framework for discerning molecular architectures residing within regional minima of energy landscapes. These minima encapsulate molecular conformations stabilized within the designated force field, wherein molecular motion manifests as intricately orchestrated vibrations and interplays among these steadfast conformations. As a corollary, techniques facilitating the attainment of the global energy minimum and various low-energy states, alongside methodologies addressing both local and global energy optimization, are frequently delineated [45, 46]

At reduced thermodynamic conditions, the manifestation of diminished energy configurations is customary within molecular entities, exerting discernible influences on their inherent characteristics. Employing methodologies characterized by determinism, either discretely or continuously, such as the Metropolis-Hastings algorithm, alternative Monte Carlo approaches, and simulated annealing procedures, proves conducive to the pursuit of global optimization [46].

Due to the quantized nature of bond vibrations in compounds such as fluorouracil and azathioprine, attempts to use the Monte Carlo method to accurately simulate and reconstruct thermodynamic properties, such as heat capacity or entropy, for chemical compounds alone do not work [47]. Hence, the use of quantum mechanics along with molecular mechanics and the Monte Carlo method is necessary.

Techniques from quantum mechanics may be used to understand electrochemical processes as well as atomic and molecular structures. The frontier molecular orbitals of each molecule were thoroughly studied using the 6-31+G* basis set and the B3LYP method [29, 48]. Tables 1 and 2 summarize the results for the compounds, consisting of EHOMO, ELUMO, and the HOMO-LUMO energy gap (Eg). The electron transfer rate of each compound is reflected in the energy gap (Eg), which indicates that the higher the electron transfer rate, the smaller the difference between donor and acceptor orbitals [43].

The two primary molecular orbitals are the minimum unoccupied molecular orbital (LUMO) and the maximum occupied molecular orbital (HOMO). The capacity to provide electrons is shown by HOMO, while the ability to take electrons is indicated by LUMO [49]. The potential of ionization ($I=-E_{HOMO}$) and electron affinity ($A=-E_{LUMO}$) are correlated to HOMO and LUMO energies, respectively [31]. The following equations [34] were used to specify the other parameters in Tables 1 and 2.

A direct relationship between the ionization potential ($I=-E_{HOMO}$) and electron affinity ($A=-E_{LUMO}$), has been demonstrated. Using the following equations, the global hardness parameter (η), as well as an electronegativity (χ), electronic chemical potential (μ), an electrophilicity (ω), and chemical softness (S) can be calculated:

$$(\eta = I - A/2) \quad (1)$$

$$(\chi = I + A/2) \quad (2)$$

$$(\mu = -(I + A)/2) \quad (3)$$

$$(\omega = \mu^2/2\eta) \quad (4)$$

$$(S = 1/2\eta) \quad (5)$$

The HOMO energy value of the FLU-SWCNT complex is about 0.26777 eV and the HOMO energy value of the FLU-BNNT complex is about -0.30095 eV (Table 1) (Figure 3).

On the other hand, the LUMO energy value of the FLU-SWCNT complex shows about -0.22780 eV, while the LUMO energy of the FLU-BNNT complex shows about -0.17633 eV. Based on this, it can be said that the greater the distance between the HOMO and LUMO orbitals, the more energy is needed to transfer electrons between these two levels, so electron transfer becomes more difficult.

The stability of a molecule is elucidated by the energy gap existing between HOMO and LUMO levels, where a broader gap signifies greater stability. The energy gap values for the FLU-SWCNT complex and the FLU-BNNT complex in this instance are 0.03997 eV and 0.12462 eV, respectively, indicating the superior stability of the FLU-BNNT complex over the carbon nanotube complex. The energy gap (Eg) of Fluorouracil with SWCNT and BNNT is shown through density of states (DOS) diagrams[50, 51] in Figure 3 (Table 1).

Cross-correlation between HOMO and LUMO energies shows an inverse relationship with ionization potential (I) and electron affinity (A). The results show that the FLU-BNNT

complex has a higher ionization potential (I). On the contrary, the FLU-SWCNT complex shows more electron affinity. Therefore, it can be said that the FLU-BNNT complex has a greater tendency to lose electrons than the FLU-SWCNT. Also, the FLU-SWCNT complex has more electron affinity than the FLU-BNNT (Table 1).

The molecular rigidity and reactivity of a species are encapsulated by its aggregate hardness parameter (η). The total hardness parameter of the FLU-BNNT complex is equal to 0.21279 eV, which indicates a lower tendency to engage in chemical processes compared to the FLU-SWCNT complex, which has a total hardness of 0.15387 eV.

Enhanced stability is intricately linked to augmented chemical hardness and energy gap magnitudes, whereas a nexus exists between reduced stability and diminished energy gap and hardness values. It is predicted that a compound that shows a lower hardness value will appear softer and therefore more polarizable and require less energy for reactivity.

More validity of hardness and stability of the FLU-BNNT complex compared to the FLU-SWCNT complex is confirmed through softness parameters (S). The values related to the softness parameter (S) for FLU-SWCNT and FLU-BNNT complexes are 3.2494 eV and 2.3497 eV, respectively. A molecule's capacity to take in electrons is increased by a greater electrophilicity index (ω). The carbon nanotube and boron nitride nanotube have electrophilicity indices of 0.19951 eV and 0.13279 eV, respectively. These quantities indicate that the carbon nanotube has a higher electrophilicity and, thus, a larger electron-accepting capacity.

One such metric to assess nanotubes is the dipole moment (DM). Higher dipole moments are an appropriate indicator of electrostatic energy and the asymmetric character of molecules. The asymmetric character of boron nitride nanotubes is demonstrated by the dipole moment of 6.5885 (Debye) for fluorouracil and boron nitride nanotubes compared to 6.4031 (Debye) for fluorouracil and carbon nanotubes.

Table 2 shows the values of electron affinity (A), total hardness (η), total softness (S) and electrophilicity (ω) of azathioprine, AZA-SWCNT and AZA-BNNT. AZA-BNNT has the highest ionization potential (I) of about 0.26517 eV compared to AZA-SWCNT. The electron affinity parameter of AZA-SWCNT is about 0.20422 eV, which indicates that AZA-SWCNT has a greater tendency to accept electrons (Table 2).

Electronegativity is shown as (χ). It should be noted that AZA-BNNT has a higher electronegativity value than AZA-SWCNT, which are 0.354315 eV and 0.30857 eV, respectively. Unlike AZA-SW, which has a total hardness value of 0.10435 eV, the AZA-BNNT composite achieves a maximum total hardness value of 0.176025 eV, which indicates the greater stability of the AZA-BNNT complex.

These results (QM) show that boron nitride nanotubes may be suitable as carriers for fluorouracil and azathioprine drugs for delivery to target cells.

Table 1. The electronic characteristics of Fluorouracil, wherein the computational assessment was conducted employing the B3LYP/6-31+G* theoretical framework.

Property	FLU	FLU- SWCNT	FLU- BNNT
HF (Hartree)	-514.0651236	-4312.9411629	8692.3215
Zero-point correction (Hartree)	0.078727	0.915490	1.4109
Thermal correction to Energy (Hartree)	0.085806	0.972677	1.526
Thermal correction to Enthalpy (Hartree)	0.086750	0.971633	1.415
Thermal correction to Gibbs Free Energy (Hartree)	0.046956	0.909835	1.4038
Sum of electronic and zero-point Energies (Hartree)	-513.986396	-4312.025673	7735.314
Sum of electronic and thermal Energies (Hartree)	-513.979318	-4311.968486	7734.015
Sum of electronic and thermal Enthalpies (Hartree)	-513.978374	-4311.967541	7734.0141
Sum of electronic and thermal Free Energies (Hartree)	-514.018167	-4312.105254	7735.4801
E (Thermal) (KCal.Mol)	53.844	610.364	954.816
CV (Cal.Mol-Kelvin)	26.465	270.289	417.499
S (Cal.Mol-Kelvin)	83.753	289.840	437.65
Dipole moment (Debye)	4.9191	6.4031	6.521
Point Group	C1	C1	C1
EHOMO (eV)	-0.29437	-0.26777	-0.30095
ELUMO (eV)	-0.15086	-0.22780	-0.17633
Eg (eV)	0.13577	0.03997	0.12462
I (eV)	0.29437	0.26777	0.30095
A (eV)	0.1586	0.22780	0.17633
χ (eV)	0.37367	0.38167	0.38911
η (eV)	0.21507	0.15387	0.21279
μ (eV)	-0.226485	-0.247785	-0.23864
ω (eV)	0.11925	0.199510	0.13279
S (eV)	2.32482	3.249496	2.3497

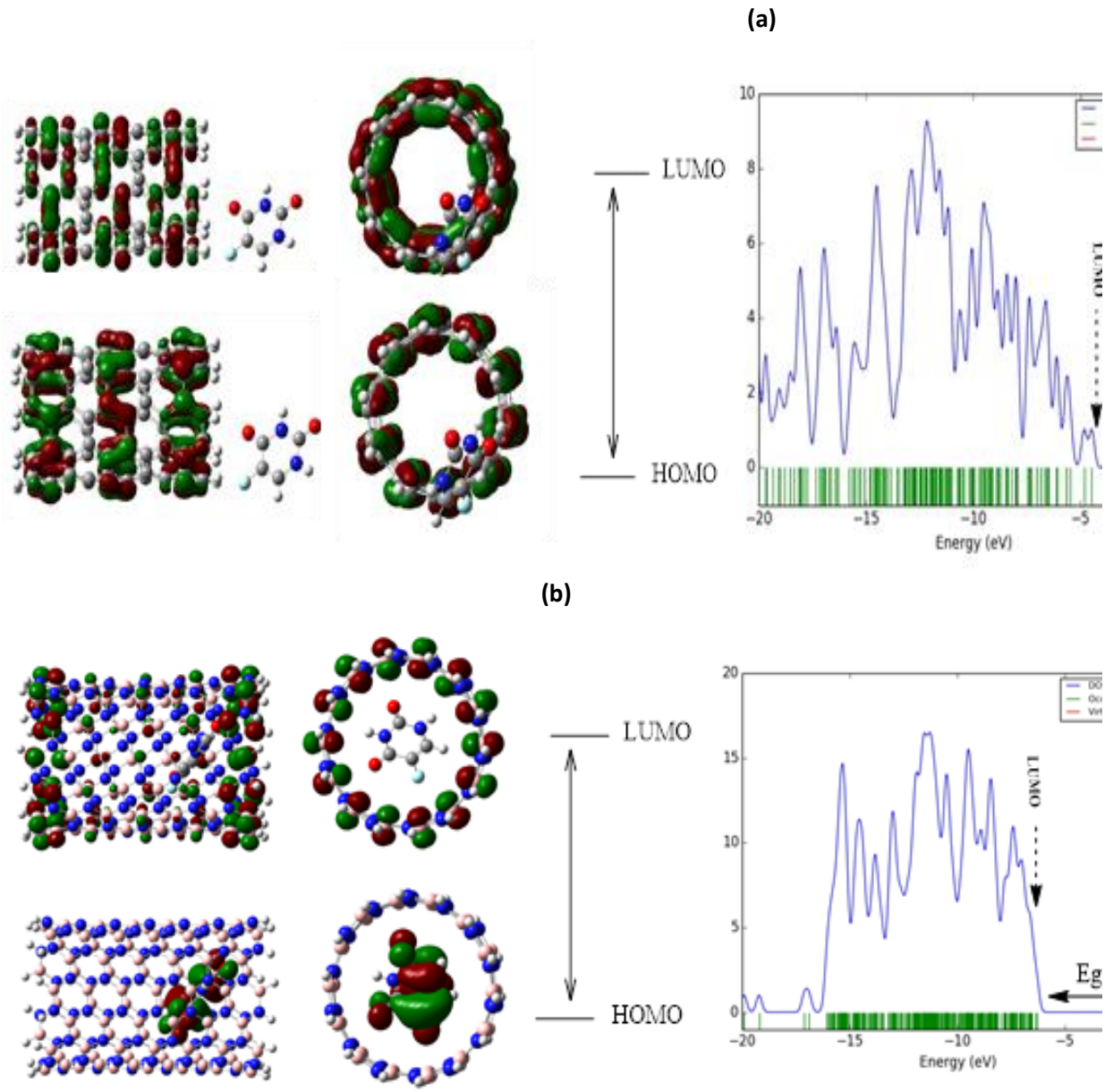

Fig. 3. Calculated Frontier molecular orbitals and DOS plots [40] of Fluorouracil with SWCNT (a) and BNNT (b) (Eg: Energy gap between LUMO and HOMO)

Table 2. The electronic characteristics of Azathioprine, wherein the computational assessment was conducted employing the B3LYP/6-31+G* theoretical framework.

Property	AZA	AZA- SWCNT	AZA- BNNT
HF (Hartree)	-1278.9	4125.1025	-8504.4829909
Zero-point correction (Hartree)	0.177847	1.0125	1.508016
Thermal correction to Energy (Hartree)	0.193524	1.07	1.624600
Thermal correction to Enthalpy (Hartree)	0.194468	1.1	1.625545
Thermal correction to Gibbs Free Energy (Hartree)	0.131914	0.90	1.379026
Sum of electronic and zero-point Energies (Hartree)	-1278.812484	5079.6859	-8502.974975
Sum of electronic and thermal Energies (Hartree)	-1278.796807	5079.4576	-8502.858390
Sum of electronic and thermal Enthalpies (Hartree)	-1278.795862	5079.4512	-8502.857446
Sum of electronic and thermal Free Energies (Hartree)	-1278.858416	5080.0121	-8503.103965
E (Thermal) (KCal.Mol)	121.438	675.476	1019.452
CV (Cal.Mol-Kelvin)	57.509	296.572	528.628
S (Cal.Mol-Kelvin)	131.656	371.632	518.842
Dipole moment (Debye)	9.3667	4.2363	4.3616
Point Group	C1	C1	C1
EHOMO (eV)	-0.2649	-0.20646	-0.26517
ELUMO (eV)	-0.16471	-0.20422	-0.17829
Eg (eV)	0.10019	0.00224	0.08688
I (eV)	0.2649	0.20646	0.26517
A (eV)	0.16471	0.20422	0.17829
χ (eV)	0.347255	0.30857	0.354315
η (eV)	0.182545	0.10435	0.176025
μ (eV)	0.214805	-0.20534	-0.22173
ω (eV)	0.126382	0.20201	0.139650
S (eV)	2.73905	4.7915	2.84050

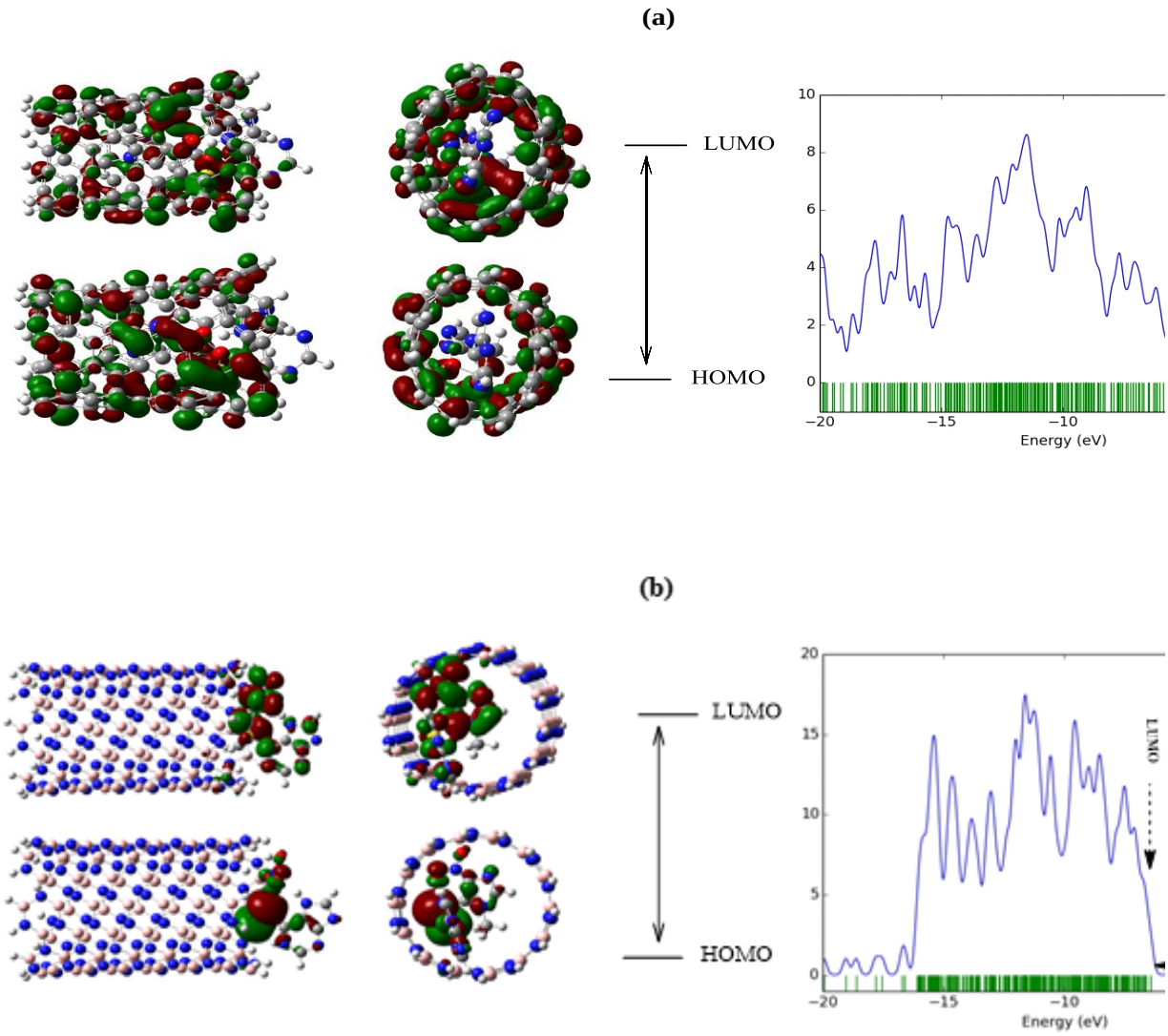

Fig. 4. Calculated Frontier molecular orbitals and DOS plots [40] of Azathioprine with SWCNT (a) and BNNT (b) (Eg: Energy gap between LUMO and HOMO)

The results obtained from molecular mechanics calculations and Monte Carlo simulation is shown in Tables 3-10 and S1-S8. The values of kinetic energy were obtained from temperatures 298 to 316 in the gas phase and solvents water, methanol, and ethanol and force fields AMBER, CHARMM, MM+, and OPLS (Tables 3 – 10 and S1 - S8). Diagrams of kinetic energy in terms of temperature are shown in Figures 5 and 8. The obtained results indicated that the kinetic energy has increased slightly (Figures 5, 8, S1 and S4).

Changes in kinetic energy at different temperatures are linear. At any given temperature and across diverse force fields, the kinetic energy remains invariant (Fig 5, 8, S1 and S8).

Notably, water exhibits superior kinetic energy compared to alternative solvents, manifesting a hierarchical sequence of motion energy levels, namely water, dimethyl sulfoxide (DMSO), ethanol, methanol, and gas phase states from highest to lowest. The congruence in the general trend of total energy and potential energy is observed across all four force fields and their respective combinations (Fig 6-7, 9 -10, S2-S3 and S5 - S6). Initially, the potential energy attains substantial magnitudes and subsequently undergoes a decline contingent on the solvent type, featuring variable slopes. In all four force fields, the potential energy descends concomitantly with escalating temperatures. A more comprehensive elucidation is presented in subsequent analysis.

The deduction can be drawn that the diminishing potential energy across diverse domains exerts the most pronounced influence on the aggregate energy state, given the linear ascension in kinetic energy across all domains contingent upon temperature, while the total energy manifestation across these domains follows a diminishing trajectory. Empirical evidence underscores that the MM+ force field exhibits superior continuity and convergence when juxtaposed with alternative force fields, thereby establishing its preferential suitability. The interrelationship between the energy levels of individual molecules and their thermodynamic stability is apparent, wherein lower energy levels correspond to heightened molecular stability. For instance, under the MM+ force field at 298 K, the total energy associated with the azathioprine medication complexed with carbon nanotubes is 3034.17 (kcal/mol) in an aqueous medium and 40754.93 (kcal/mol) in methanol. In a parallel scenario, the total energy of azathioprine bound to boron nitride nanotubes is 1854.128 (kcal/mol) in water and 32538.71 (kcal/mol) in methanol, as delineated in Tables 3-10. Comparative analysis of these outcomes reveals the boron nitride nanotube to exhibit lower energy, indicative of heightened stability within a water medium, as illustrated in Figures 8-10.

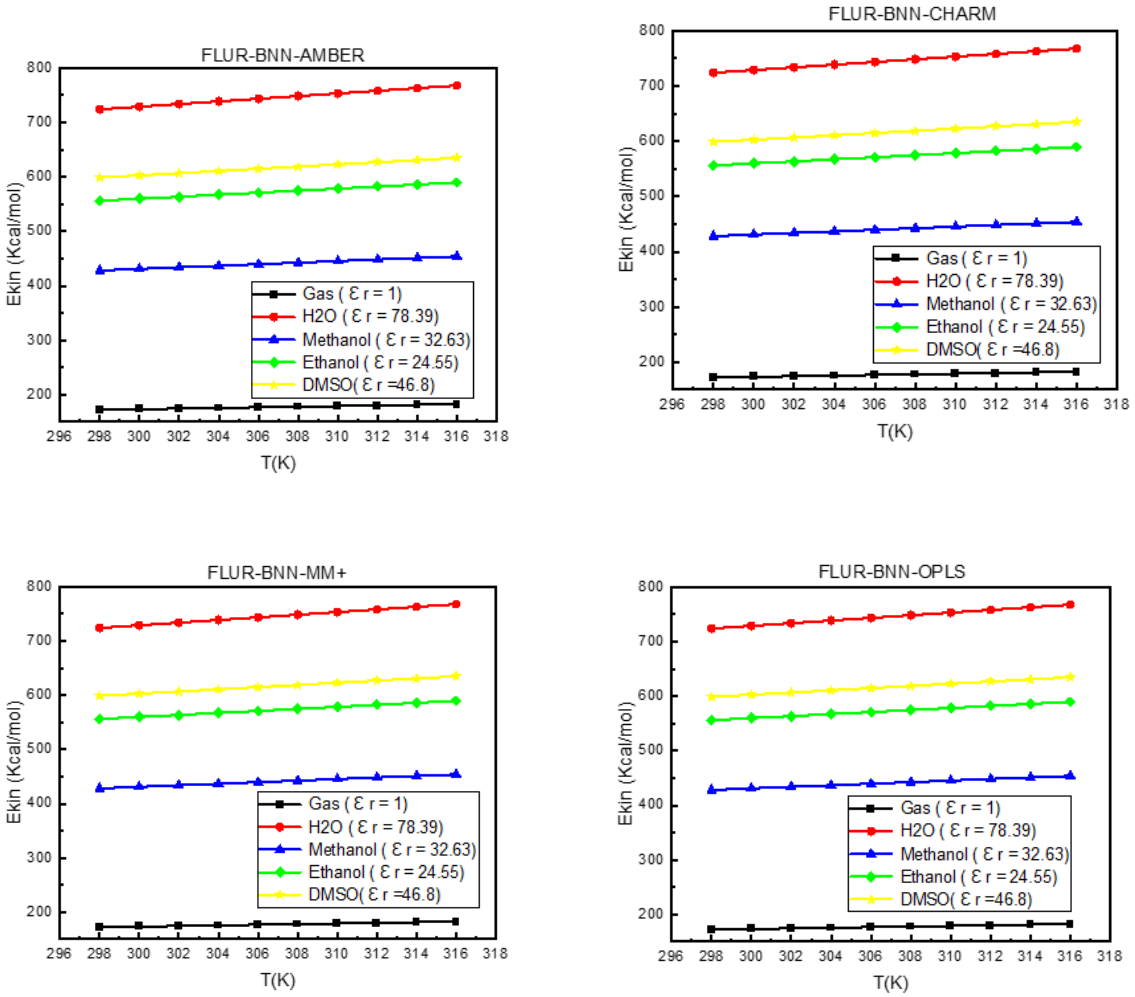

Fig. 5. Kinetic energies (E_{kin}) (kcal/mol) were calculated versus temperature at different dielectric constants through Monte Carlo simulation in the AMBER, OPLS, CHARMM, and MM+ force field for FLU- BNNT.

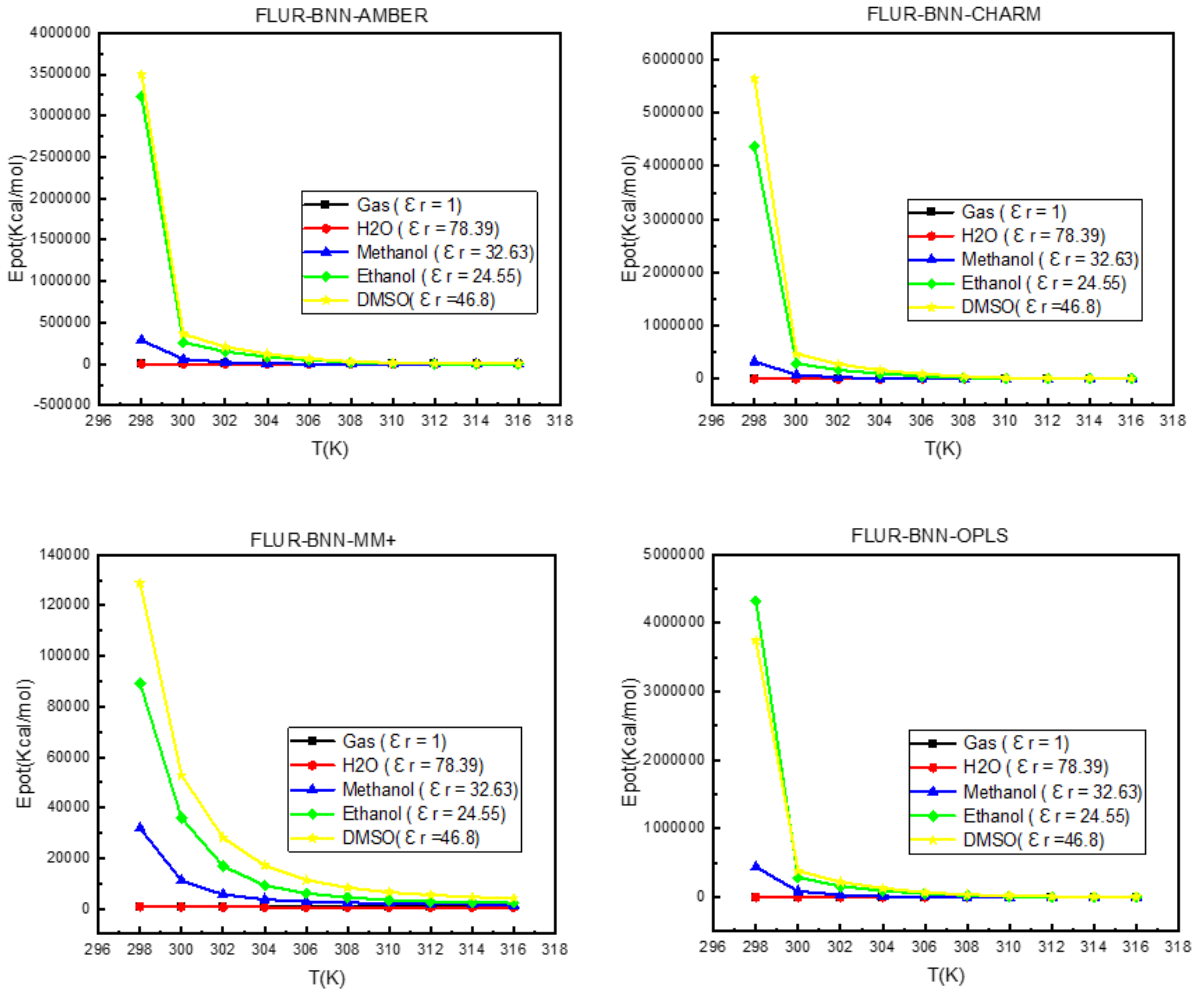

Fig. 6. Potential energies (E_{pot}) (kcal/mol) computed vs. temperature at varied dielectric constants with the aid of Monte Carlo simulation in the AMBER, OPLS, CHARMM, and MM+ force fields for FLU-BNNT

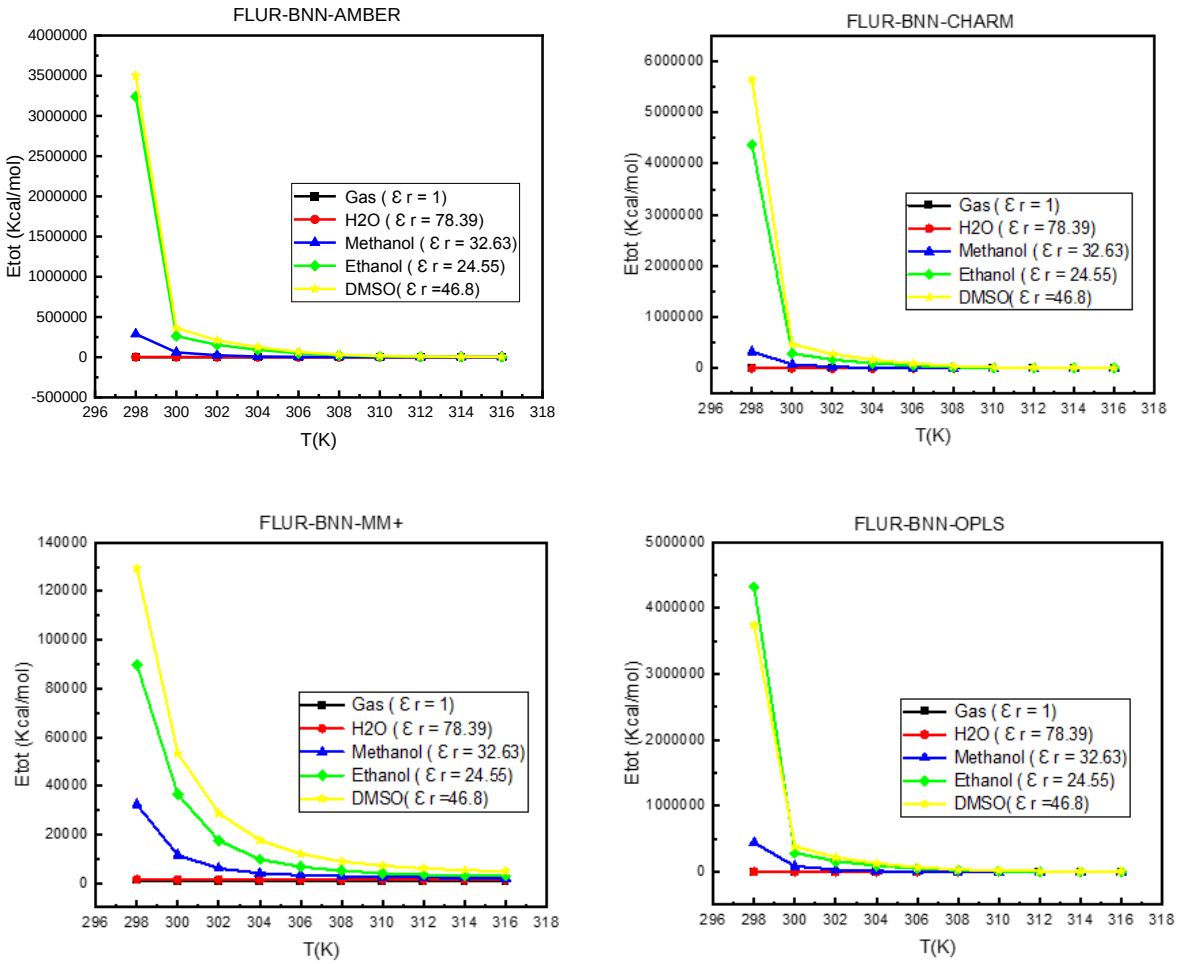

Fig. 7. Total energies (E_{Tot}) (kcal/mol) computed vs. temperature at varied dielectric constants with the aid of Monte Carlo simulation in the AMBER, OPLS, CHARMM, and MM+ force fields for FLU-BNNT

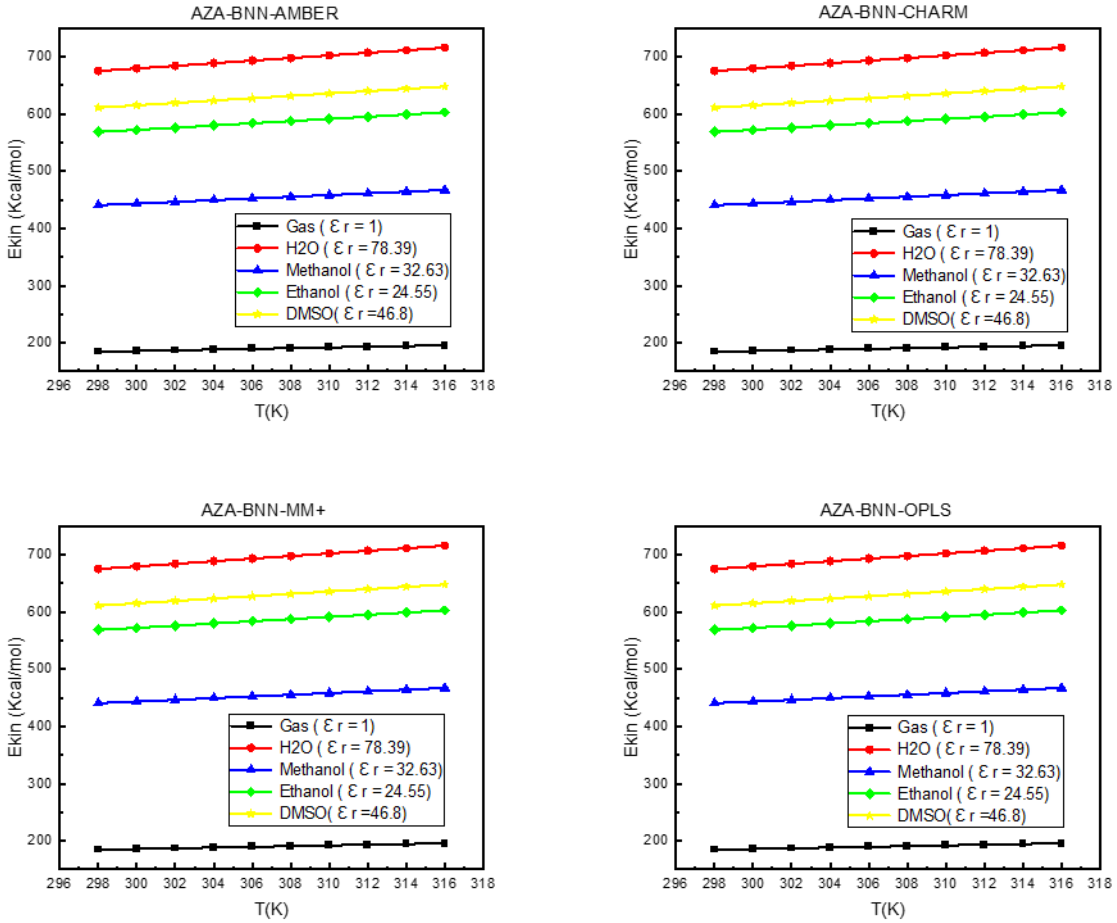

Fig. 8. Kinetic energies (E_{kin}) (kcal/mol) were calculated versus temperature at different dielectric constants through Monte Carlo simulation in the AMBER, OPLS, CHARMM, and MM+ force fields for AZA- BNNT.

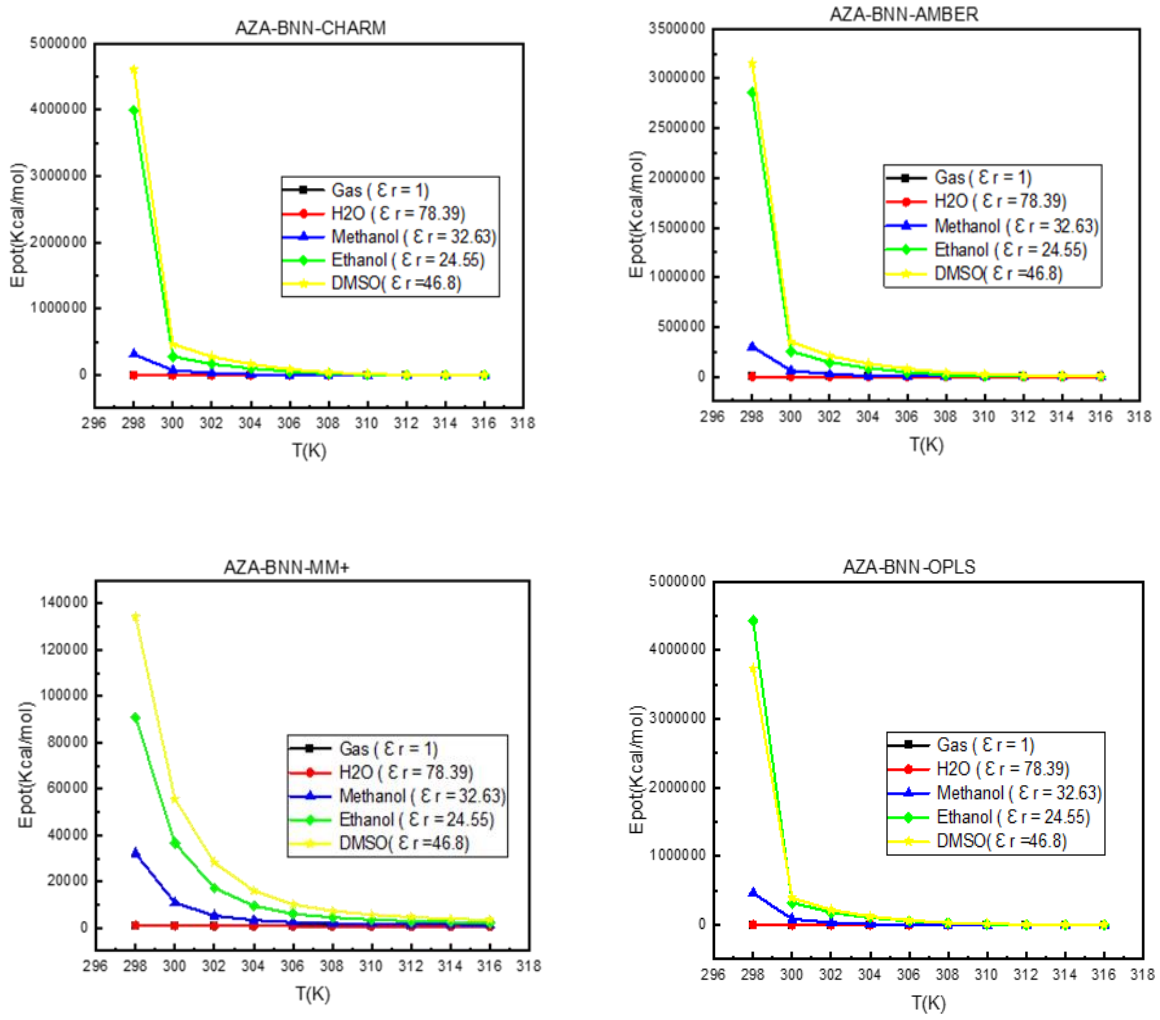

Fig. 9. Potential energies (E_{pot}) (kcal/mol) were calculated versus temperature at different dielectric constants through Monte Carlo simulation in the AMBER, OPLS, CHARMM, and MM+ force fields for AZA- BNNT.

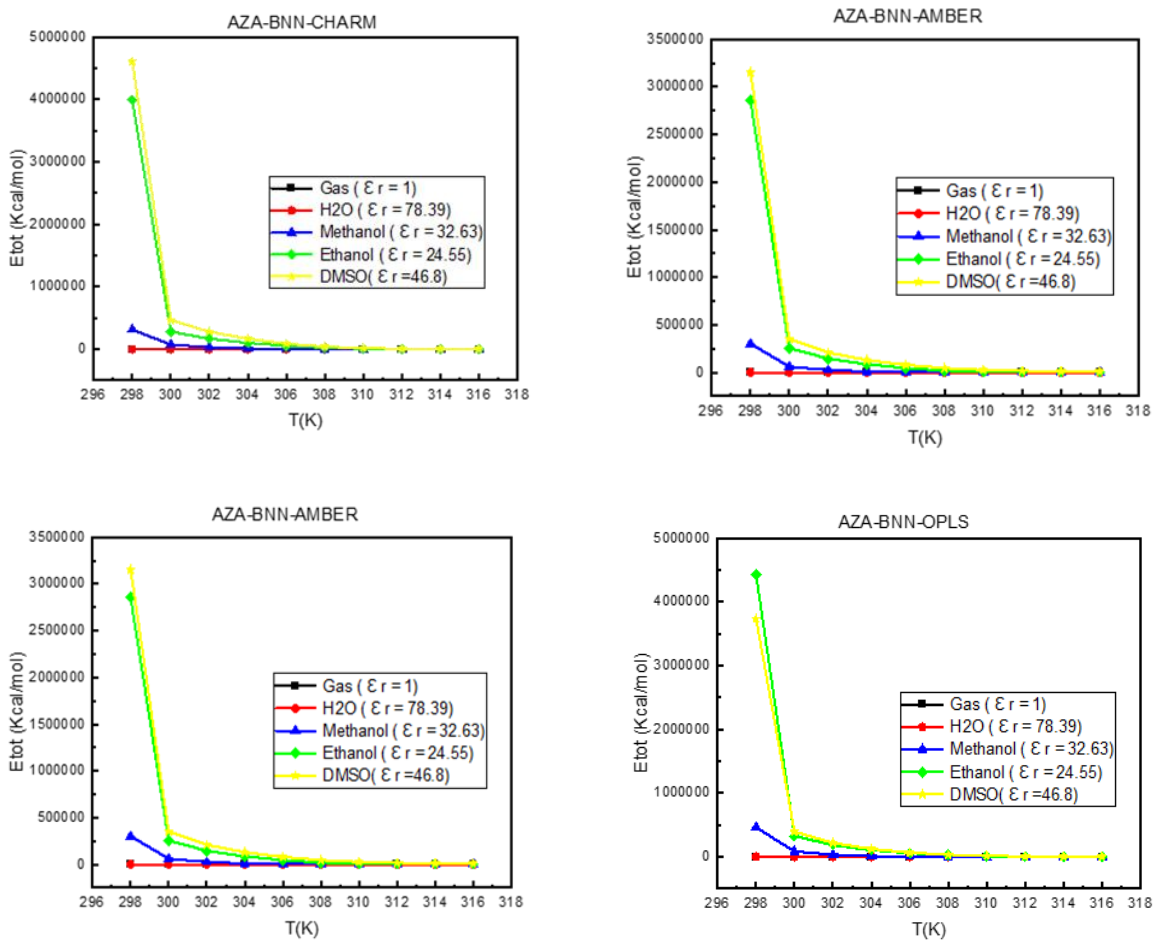

Fig. 10. Total energies (E_{tot}) (kcal/mol) calculated versus temperature at different dielectric constants through Monte Carlo simulation in the AMBER, OPLS, CHARMM, and MM+ force field for AZA- BNNT.

4. Conclusion

Thermodynamic characteristics and molecular frontier orbitals (FMOs) of various substances were examined. Analysis was done on molecular structure parameters such as electrophilicity (ω), chemical hardness (η), electronic chemical potential (μ), ionization potential (I), and electron affinity (A). The increased stability of the FLU-BNNT complex is validated by the energy of HOMO, LUMO, and Gibbs findings. In addition, the results show that the AZA-BNNT complex is more stable, which is supported by the HOMO and LUMO energy values?

The gas phase interactions between fluorouracil (FLU) and azathioprine (AZA) with single-walled carbon nanotubes (SWCNTs) and boron nitride nanotubes (BNNTs) were assessed through the utilization of density functional theory (DFT) computations. Employing the DFT methodology, the influence of diverse solvents on the interplay between FLU and AZA molecules and SWNT and BNNT within the self-consistent reaction field Onsager model (SCRF) was additionally scrutinized. Moreover, the impact of temperature on the stability of molecular associations in various solvents was probed. The density of states (DOS), frontier molecular orbitals (FMOs), and thermodynamic attributes of the entities under investigation were scrutinized in these calculations. Furthermore, attributes of molecular structure, encompassing ionization potential (I), electron affinity (A), chemical hardness (η), electronic chemical potential (μ), and electrophilicity (ω), were also examined. The results showed that the stability of the FLU-BNNT complex is confirmed by the energy difference between occupied molecular orbital (HOMO) and unoccupied molecular orbital (LUMO) and also Gibbs free energy values. In addition, the findings show that the AZA-BNNT complex shows more stability than AZA-SWCNT, which is determined by the energy difference between occupied molecular orbital (HOMO) and unoccupied molecular orbital (LUMO) and also Gibbs free energy values.

Molecular dynamics simulations employing molecular mechanics and quantum mechanical calculations were conducted to scrutinize the impact of diverse solvents and temperatures on Fluorouracil (FLU) and Azathioprine (AZA) in conjunction with Single-Walled Carbon Nanotubes (SWNTs) and Boron Nitride Nanotubes (BNNTs). An assessment of energy variations derived from the AMBER, OPLS, CHARM (Bio+), and MM+ force fields was performed to discern alterations in force fields. Noteworthy modifications in solvents and force fields ensued due to shifts in solvation-free energy within non-polar solvents. However, it is imperative to note that modifications in the free energy of solvation within more polar

liquids do not solely arise from fluctuations in atomic charges, and the practical comparability of the four force fields is not guaranteed. The consideration of nonpolar molecules as solutes introduces a significant degree of variability. The equilibrium between the charges of polar molecules and interaction parameters dictates the strength and configuration of pertinent polar interactions. Methanol exhibited the lowest kinetic energy (Ekin) value in graphs, denoting its status as the most stable solvent for simulation. In contrast, water displayed the smallest numerical value in potential energy (Epot) graphs, establishing it as the most stable and suitable solvent for simulation, as its energy value constituted the lowest contribution to total energy (Etot). On the other hand, water shows the lowest numerical value in the potential energy diagrams (Epot) and introduces it as the most stable and suitable solvent for simulation, because the potential energy has the greatest impact on the total energy (Etot). Simulations involving the interaction of FLU-BNNT complex in water, DMSO, methanol, and ethanol demonstrated consistent outcomes across OPLS, CHARM, and AMBER force fields, while notable disparities emerged in MM+ force field computations, precisely represented by the separation between graphs in the MM+ force field.

The results for the AZA-BNNT complex and FLU-BNNT complex were quite similar. The most stable solvent in the force fields of CHARM, OPLS, and AMBER was water. By examining the complexes of FLU and AZA drugs attached to SWNT and BNNT nanocarriers, it was found that MM+ has the lowest energy value and is the best field for performing calculations.

The present conclusions are likewise in agreement with the results of calculations based on quantum mechanics. BNNTs are better carriers for AZA and FLU. Consequently, the outcomes of quantum mechanics, molecular mechanics, and Monte Carlo simulations are warranted. Nanotechnology has advanced significantly with the use of SWNTs and BNNTs

for the delivery of anticancer medicines. Chemotherapy drugs used in conventional cancer treatment may have negative effects on healthy tissues. Therefore, to administer anticancer medications, effective drug delivery systems based on CNTs must be developed. Despite its relative development, there are still several obstacles in the way of clinical uses for nanotechnology.

On the other hand, SWCNT and BNNT-based drug delivery systems offer a potential means of delivering anticancer medications to specific organs or tissues. This review article's observations and findings suggested that drug delivery systems based on BNNTs and SWNTs would be extremely successful and capable of producing enough empirical evidence to warrant clinical use.

Availability of Data

The data that support this study are available in the article and accompanying online supplementary material.

Acknowledgments

The authors are thankful to the Ahvaz Branch of Islamic Azad University and Zanjan Branch of Islamic Azad University for partial support of this work.

References:

[1] L. C. Kennedy, L. R. Bickford, N. A. Lewinski, A. J. Coughlin, Y. Hu, E. S. Day, J. L. West, R. A. Drezek, Small, 7 (2011) 169-183

[2] J. Guo, L. Bourre, D. M. Soden, G. C. O'Sullivan, C. O'Driscoll, Biotechnol. Adv., 29 (2011) 402-417

[3] M. Bartkowski, S. Giordani, Dalton Transactions, 50 (2021) 2300-2309

[4] T. A. Hilder, J. M. Hill, Nanotechnology, 18 (2007) 275704

[5] X. Liu, Y. Ying, J. Ping, Biosens. Bioelectron., 167 (2020) 112495

[6] P. Eskandari, Z. Abousalman-Rezvani, H. Roghani-Mamaqani, M. Salami-Kalajahi, Adv. Colloid Interface Sci., 294 (2021) 102471

[7] M. Riaz, Pak. J. Pharm. Sci., 9 (1996) 65-77.

[8] G. Peters, C. Van der Wilt, C. Van Moorsel, J. Kroep, A. Bergman, S. Ackland, Pharmacol. Ther., 87 (2000) 227-253

[9] G. E. TAGATZ, R. L. SIMMONS, *Pregnancy after renal transplantation*. 1975, American College of Physicians. p. 113-114.

[10] J. S. Maltzman, G. A. Koretzky, The Journal of clinical investigation, 111 (2003) 1122-1124.

[11] J. Saam, G. C. Critchfield, S. A. Hamilton, B. B. Roa, R. J. Wenstrup, R. R. Kaldate, Clinical colorectal cancer, 10 (2011) 203-206

[12] A. Elhissi, W. Ahmed, I. U. Hassan, V. Dhanak, A. D'Emanuele, J. Drug Delivery, 2012 (2012)

[13] I. Marijanović, M. Kraljević, D. Bevanda Glibo, T. Buhovac, E. Černi Obrdalj, Psychiatria Danubina, 33 (2021) 89-96.

[14] A. T. Jalil, A. H. D. Al-Khafaji, A. Karevskiy, S. H. Dilfy, Z. K. Hanan, *WITHDRAWN: Polymerase chain reaction technique for molecular detection of HPV16 infections among women with cervical cancer in Dhi-Qar Province*. 2021, Elsevier.

[15] Z. Yu, Y. Zhao, B. Hong, Z. Jin, J. Huang, D. Cai, X.-S. Hua, IEEE Transactions on Multimedia, 24 (2021) 4482-4492

[16] I. Marijanović, D. Bevanda Glibo, T. Lasić, M. Kraljević, T. Buhovac, T. Cerić, E. Sokolović, Psychiatria Danubina, 33 (2021) 304-307.

[17] D. Franjić, D. Babić, I. Marijanović, M. Martinac, Psychiatria Danubina, 33 (2021) 297-303.

[18] M. Kordić, V. Dragišić, N. Šutalo, J. Mišković, I. Klupke Sarić, A. Bogut, M. Karin, Psychiatria Danubina, 33 (2021) 97-98.

[19] K. Shayan, A. Nowroozi, Appl. Surf. Sci., 428 (2018) 500-513

[20] M. Gomar, S. Yeganegi, Microporous Mesoporous Mater., 252 (2017) 167-172

[21] M. Shahabi, H. Raissi, J. Mol. Model., 25 (2019) 304

[22] N. G. Chopra, R. Luyken, K. Cherrey, V. H. Crespi, M. L. Cohen, S. G. Louie, A. Zettl, science, 269 (1995) 966-967

[23] A. Oberlin, M. Endo, T. Koyama, J. Cryst. Growth, 32 (1976) 335-349

[24] M. Frisch, G. Trucks, H. Schlegel, G. Scuseria, M. Robb, J. Cheeseman, G. Scalmani, V. Barone, B. Mennucci, G. Petersson, Uranyl Extraction by N, N-Dialkylamide Ligands Studied by Static and Dynamic DFT Simulations, in Gaussian 09. Gaussian Inc Wallingford, 2009.

[25] D. Nori-Shargh, H. Yahyaei, M. Jafari, S. Rafatpanah, A. M. Tazekand, S. N. Mousavi, R. Shakibazadeh, Phosphorus Sulfur Silicon Relat. Elem., 186 (2011) 1538-1553

[26] A. Frisch, A. Nielson, A. Holder, Gaussian Inc., Pittsburgh, PA, 556 (2000).

[27] Y. Shao, L. F. Molnar, Y. Jung, J. Kussmann, C. Ochsenfeld, S. T. Brown, A. T. Gilbert, L. V. Slipchenko, S. V. Levchenko, D. P. O'Neill, Phys. Chem. Chem. Phys., 8 (2006) 3172-3191

[28] N. Saikia, R. C. Deka, Comput. Theor. Chem., 964 (2011) 257-261

[29] V. Khodadadi, N. Hasanzadeh, H. Yahyaei, A. Rayatzadeh, J. Chil. Chem. Soc., 66 (2021) 5365-5379

[30] M. Kastner, Commun. Nonlinear Sci. Numer. Simul., 15 (2010) 1589-1602

[31] F. Buonocore, F. Trani, D. Ninno, A. Di Matteo, G. Cantele, G. Iadonisi, Nanotechnology, 19 (2007) 025711

[32] H. Yahyaei, M. Monajjemi, H. Aghaie, K. Zare, J. Comput. Theor. Nanosci., 10 (2013) 2332-2341

[33] R. HyperChem, *7.0 for windows, Hypercube*. 2002, Inc.

[34] W. D. Cornell, P. Cieplak, C. I. Bayly, I. R. Gould, K. M. Merz, D. M. Ferguson, D. C. Spellmeyer, T. Fox, J. W. Caldwell, P. A. Kollman, Journal of the American Chemical Society, 117 (1995) 5179-5197

[35] A. MacKerell Jr, Evanseck JD, Field MJ, Fischer S, Gao J, Guo H, Ha S, Joseph-McCarthy D, Kuchnir L, Kuczera K, Lau FTK, Mattos C, Michnick S, Ngo T, Nguyen DT, Prodhom B, Reiher WE III, Roux B, Schlenkrich M, Smith JC, Stote R, Straub J, Watanabe M, Wiórkiewicz-Kuczera J, Yin D, Karplus MJ Phys. Chem. B, 102 (1998) 3586

[36] E. Neria, S. Fischer, M. Karplus, J. Chem. Phys, 105 (1996) 1902-1921

[37] W. L. Jorgensen, J. Tirado-Rives, J. Am. Chem. Soc, 110 (1988) 1657-1666

[38] M. H. Jamshidi, N. Hasanzadeh, H. Yahyaei, A. Bahrami, Lett. Org. Chem., 20 (2023) 657-671

[39] A. Szczepanska, J. L. Espartero, A. J. Moreno-Vargas, A. T. Carmona, I. Robina, S. Remmert, C. Parish, J. Org. Chem., 72 (2007) 6776-6785

[40] W. K. Hastings, Biometrika, 57 (1970) 97-109

[41] J. S. Liu, F. Liang, W. H. Wong, J. Am. Stat. Assoc., 95 (2000) 121-134

[42] D. N. Theodorou, Industrial & engineering chemistry research, 49 (2010) 3047-3058

[43] L. Lacerda, S. Raffa, M. Prato, A. Bianco, K. Kostarelos, Nano Today, 2 (2007) 38-43.

[44] M. E. Davis, Z. G. Chen, D. M. Shin, Nat Rev Drug Discov, 7 (2008) 771-782

[45] M. E. Davis, Z. Chen, D. M. Shin, Nature reviews Drug discovery, 7 (2008) 771-782.

[46] B. Kuhn, P. A. Kollman, Journal of medicinal chemistry, 43 (2000) 3786-3791.

[47] S. Huo, I. Massova, P. A. Kollman, J. Comput. Chem., 23 (2002) 15-27

[48] C. Lee, W. Yang, R. Parr, (1988).

[49] J.-i. Aihara, Phys. Chem. Chem. Phys., 2 (2000) 3121-3125

[50] N. M. O'boyle, A. L. Tenderholt, K. M. Langner, J. Comput. Chem., 29 (2008) 839-845

[51] N. O'Boyle, *GaussSum, Version 2.0. 5, 2007*.